

Is the magnetic field in the heliosheath laminar or a turbulent bath of bubbles?

M. Opher¹

Astronomy Department, Boston University, 725 Commonwealth Avenue, Boston, MA

mopher@bu.edu

J. F. Drake²

University of Maryland, College Park, MD

M. Swisdak³

University of Maryland, College Park, MD

K. M. Schoeffler³

University of Maryland, College Park, MD

J. D. Richardson⁴

Kavli Institute for Astrophysics and Space Research, Massachusetts Institute of
Technology, Cambridge, MA

R. B. Decker⁵

John Hopkins Univ., Applied Physics Lab., Laurel MD

G. Toth⁶

University of Michigan, Ann Arbor, MI

Received _____; accepted _____

ABSTRACT

All the current global models of the heliosphere are based on the assumption that the magnetic field in the heliosheath, in the region close to the heliopause is laminar. We argue that in that region the heliospheric magnetic field is not laminar but instead consists of magnetic bubbles. We refer to it as the bubble-dominated heliosheath region. Recently, we proposed that the annihilation of the “sectorized” magnetic field within the heliosheath as it is compressed on its approach to the heliopause produces the anomalous cosmic rays and also energetic electrons. As a product of the annihilation of the sectorized magnetic field, densely-packed magnetic islands (that further interact to form magnetic bubbles) are produced. These magnetic islands/bubbles will be convected with the ambient flows as the sector region is carried to higher latitudes filling the heliosheath. We further argue that the magnetic islands/bubbles will develop upstream within the heliosheath. As a result, the magnetic field in the heliosheath sector region will be disordered well upstream of the heliopause. We present a 3D MHD simulation with very high numerical resolution that captures the north-south boundaries of the sector region. We show that due to the high pressure of the interstellar magnetic field a north-south asymmetry develops such that the disordered sectorized region fills a large portion of the northern part of the heliosphere with a smaller extension in the southern hemisphere. We suggest that this scenario is supported by the following changes that occur around 2008 and from 2009.16 onward: a) the sudden decrease in the intensity of low energy electrons (0.02-1.5 MeV) detected by Voyager 2 ; b) a sharp reduction in the intensity of fluctuations of the radial flow; and c) the dramatic differences in intensity trends between galactic cosmic ray electrons (3.8-59 MeV) at Voyager 1 and 2. We argue that these observations are a consequence of Voyager 2 leaving the sector region of disordered field during

these periods and crossing into a region of unipolar laminar field.

Subject headings: interplanetary medium – ISM:kinematics and dynamics – MHD:solar
wind – Sun:magnetic fields

1. Introduction

The current understanding of the outer heliosphere has changed dramatically in the last few years due to the recent observations of Voyager 1 and 2 (Stone et al. 2005, 2008) and IBEX (McComas et al. 2009). The Voyager data at the crossing of the termination shock (TS) revealed that the anomalous cosmic rays (ACRs) were not accelerated at the location of the spacecraft. Several scenarios were suggested to explain these surprising observations: the ACRs could be accelerated by the TS along the flanks of the heliosphere (McComas & Schwadron 2006), in the heliosheath by compressional turbulence (Fisk & Gloeckler 2006, 2007, 2009) or by reconnection in the sectorized field near the heliopause (Lazarian & Opher 2009, Drake et al. 2010). Another shift in paradigm occurred when it became clear that the pickup ions carry a large portion of the plasma energy (Zank et al. 1999, Richardson et al. 2008). Finally the data from IBEX revealed a ribbon of energetic neutral atoms (ENAs), suggesting that the interstellar magnetic field has a very important role in shaping the heliosphere. This result reinforces the earlier Voyager observations: the interstellar magnetic field produces a north-south asymmetry in the location of the termination shock (Opher et al. 2006, 2009).

Recently, we suggested a new mechanism for the acceleration of the ACRs. We suggested that the sectorized heliospheric magnetic field, which results from the flapping of the heliospheric current sheet, piles up as it approaches the heliopause, narrowing the current sheets that separate the sectors, and triggering the onset of collisionless magnetic reconnection (Drake et al. 2010). We argued that reconnection is responsible for the acceleration of the ACRs and also energetic electrons.

We showed (Drake et al. 2010), using particle-in-cell (PIC) simulations, that the sectors break up into a bath of magnetic islands and that most of the magnetic energy goes into energetic ions, with significant but smaller amounts of energy going into electrons. The most

energetic ions gain energy as they reflect from the ends of contracting magnetic islands, a first-order Fermi process. The simulations also revealed that the mirror and firehose conditions play an essential role in the reconnection dynamics and particle acceleration. An analytic model was constructed in which the Fermi drive, modulated by the approach to firehose marginality, is balanced by convective loss. The ACR differential energy spectrum takes the form of a power law with a spectral index slightly above 1.5.

Here we analyze the global topology of the heliospheric current sheet (HCS) and the sector region. We argue that within the sector region but upstream of the heliopause, the heliospheric magnetic field is not laminar but instead filled with nested magnetic islands. The magnetic islands/bubbles formed during reconnection of the sector region upstream of the heliopause will be convected with the flows as the sector boundary is carried to higher latitudes, filling the heliosheath upstream of the heliopause.

We argue that due to the increased pressure of the interstellar magnetic field (Opher et al. 2006, 2007) the sector region and embedded islands are carried mostly to the northern hemisphere. We therefore predict an asymmetry of the magnetic structure between the northern and southern hemispheres and between the heliosheath sector region and the field outside of it. Therefore we predict that the northern hemisphere will be predominantly a disordered field, filled with magnetic islands and not a laminar field.

We further argue that the magnetic islands might develop upstream (but still within the heliosheath) where collisionless reconnection is unfavorable – large perturbations of the sector structure near the heliopause might cause compressions of the current sheet upstream, triggering reconnection. As a result, the magnetic field in the heliosheath sector region will be disordered well upstream of the heliopause. If this hypothesis is correct, the Voyagers may already have crossed into a region of disordered field consisting of nested magnetic islands. We present data from reconnection simulations of a sector magnetic

field, using a particle-in-cell code that, surprisingly, exhibit characteristics similar to the Voyager data: the magnetic field exhibits reversals but with a more erratic spacing than the initial state; and reconnection of the nested islands is suppressed due to the approach to the firehose marginal stability condition so plasma flows are irregular and only occasionally exhibit traditional reconnection signatures. We denote the late-time non-reconnecting magnetic islands as “bubbles” since in cross section they more closely resemble a nested volume of soap bubbles than a system of reconnecting islands.

Energetic electrons are especially sensitive to the large-scale magnetic structure of the heliosheath because of their high velocity. The presence of magnetic islands/bubbles in the heliosheath sector region will change the electron transport. Specifically a disordered heliospheric magnetic field near the heliopause acts as the window through which galactic cosmic ray electrons travelling along the interstellar magnetic fields can enter and percolate through the heliosphere. Magnetic islands/bubbles will act as local traps for these energetic electrons. Since lower energy electrons are produced during reconnection in the sectorized field in the same region, these two classes of electrons should display similar modulation characteristics. Therefore, we argue that there should be a north-south asymmetry between the electron intensities at Voyager 1 and 2 and between the intensities measured while the spacecrafts are within the bubble dominated region and outside of it.

This prediction will change our view of the heliosphere since all the current global models (e.g., Opher et al. 2006, 2009, Heerikhuisen et al. 2009, Pogorelov et al. 2009, Ratkiewicz et al. 2009) are based on the presumption that the magnetic field in the outer heliosheath close to the heliopause (HP) and in the heliosheath sector region is laminar. More recently Czechowski et al. 2010 analyzed the behaviour of the HCS in a kinematic model. They suggested that close to the HP mixed polarities could reconnect making the field random.

We present Voyager 1 and 2 data that supports this disordered field hypothesis. The Voyager 1 and 2 are moving through the sector region, are near the boundary between the sector and non-sector region, and have therefore sampled both regions.

The structure of this article is the following: in the next section we show the global behavior of a modeled sector region based on a MHD description. This will set the context for the Voyager trajectories compared with the sector region. We then present Voyager 1 and 2 observations that support our proposed scenario. We then present the results of PIC simulations of the sector region and discuss the structure of the resulting nested magnetic islands/bubbles and plasma flows. Finally, we discuss the implications of our predictions for the understanding of the current measurements by Voyager 2, and our global understanding of the heliosheath, the sector region and heliopause.

2. Global Behaviour of the Sector Boundary

Because of the tilt between the solar rotation and magnetic axis, the actual HCS oscillates up and down, producing a magnetic field with a “ballerina skirt” shape. The drop of the solar wind speed beyond the termination shock causes the sectors to compress. This behavior was demonstrated in MHD simulations in Drake et al. 2010 and with greater resolution by Borovikov et al. 2008. At the current stage in the solar cycle, the limits of the sector boundary are approximately $\pm 30^\circ$, close to the latitudes of Voyager 1 and 2.

We have carried out simulations with a sector region with a latitudinal width of 60° . We used a 3D MHD multifluid model described in Opher et al. 2009. This model is based on BATS-R-US (for a more recent description see Toth et al. 2011). Our model has five fluids (similar to Alexashov & Izmodenov (2005) and Zank et al.(1996)). In this approach there are four populations of neutral H atoms, for every region in the interaction between

the solar wind and the interstellar wind. Population 4 represents the H atoms of interstellar origin. Population 1 represents the H atoms that exist in the region between the bow shock and heliopause. Populations 3 and 2 represent the H atoms in the supersonic solar wind and in the compressed region between the termination shock and the heliopause, respectively. All four H populations are described by separate systems of the Euler equations with the corresponding source terms. Each population is created in its respective region but is free to move between the different regions as the simulation evolves. The ionized component interacts with the H neutrals via charge exchange. For more details see Opher et al. (2009). The parameters for the density, velocity and temperature for the ions and neutrals in the interstellar medium reflect the best observational values. The parameters for the inner boundary (located at 30 AU) were chosen to match those used by Izmodenov et al. (2008): proton density of $n = 8.74 \times 10^{-3} \text{cm}^{-3}$, temperature $T = 1.087 \times 10^5 \text{K}$, speed of $v = 417 \text{km/s}$ and a Parker spiral magnetic field with strength $B = 7.17 \times 10^{-3} \text{G}$ at the equator. The outer boundary conditions are $n = 0.06 \text{cm}^{-3}$, velocity equal to 26.3km/s , and $T = 6519 \text{K}$. The neutral hydrogen in the local interstellar medium is assumed to have $n = 0.18 \text{cm}^{-3}$ and the same velocity and temperature as the ionized local interstellar medium.

The interstellar magnetic field B_{ISM} intensity taken was $4.4 \mu\text{G}$ and the orientation was such that the angle between the interstellar velocity and magnetic field is 20° and the angle between the plane containing the interstellar velocity and magnetic field and the solar equator is 60° . This orientation and intensity produced the asymmetries in the termination shock locations as measured by the Voyagers (Opher et al. 2009). Matching the heliosheath flows measured by Voyager 2 requires slightly different values (Opher et al. 2009). This chosen orientation is close to the one inferred from IBEX (McComas et al. 2010) and the ones currently used based on hydrogen deflection arguments (Pogorelov et al. 2008).

We used fixed inner boundary conditions for the ion and neutral fluids. The outer boundaries were all outflows with the exception of the -x boundary, where the inflow conditions were imposed for the ionized and the population of neutrals coming from the interstellar medium (Population 4). The outer boundaries of the grid are set at $-1000AU$ and $1000AU$ in x, y, z directions, respectively. The description of the coordinate system is given in Opher et al. (2009).

To capture the sector boundary in the heliosheath adaptive mesh refinement was used. Several refinements were done throughout the computational run. The final computational cells ranges from $0.03 AU$ to $31.25 AU$. The block used had $8 \times 8 \times 8$ cells (see Toth et al. 2011). The total number of blocks was 3.0×10^6 blocks and the total number of cells was 1.4×10^9 . The simulation presented here was run for 83.2 years of simulation time on approximately 2000 CPUs. More details of this simulation and the steps involved are given in Opher et al. 2011.

Figure 1 shows the distribution of the magnitude of the magnetic field in the meridional plane (x-z plane). The sector spacing decreases downstream of the termination shock and further decreases on the approach to the heliopause. The approximate trajectories of Voyager 1 and 2 are indicated with red and blue lines, respectively. Figure 2 shows a blowup of the same meridional cut.

There is an asymmetry of the heliosphere due to the interstellar magnetic field. The inclination of the interstellar magnetic field compresses the southern hemisphere, pushing the heliopause and the termination shock in this region closer to the Sun (Opher et al. 2006, 2007, 2009). The effect of the difference in pressure between the north and south is to deflect the sector boundary to the north. Figures 1 and 2 show this effect.

We are able to resolve the alternating sectors out to the middle of the heliosheath. The sector structure is compressed downstream of the TS (the sector spacing decreases from

4.7AU to 1.9AU) and the spacing of the sectors continuously decreases further into the heliosheath as the radial plasma velocity decreases. Deep into the heliosheath resolutions finer than 0.03 *AU* are needed. In any case, the sectors close to the heliopause are expected to reconnect and possibly trigger reconnection further upstream. The decrease in spacing of the sectors is seen in Figures 2 and 3. Figure 3 presents a zoom of the sectors between the region just upstream of the termination shock into the heliosheath. The decrease of the spacing of the sectors can be seen as the solar wind crosses the termination shock. The loss of resolution deep in the heliosheath can be seen as well.

In the heliosheath the heliospheric magnetic field, to lowest order, simply adds to the dominant thermal pressure so the sector structure is not expected to alter the large-scale plasma flow pattern. Thus, we can simply follow the flow streamlines to determine what fraction of the sector region will be carried to the northern hemisphere even though the resolution is insufficient to define the sectors. This same procedure was recently followed by Czechowski et al. 2010. The white streamlines in Figure 1 show the boundary of the sector region. With increased resolution and a longer simulation time we expect the sector region to fill the domain bounded by the white streamlines. We can see that the northern sector region is much thicker than the sector region carried to the south. The thickening of the northern sector region results from the increased pressure of the interstellar magnetic field in the south, which diverts the overall heliosheath flow to the north. Thus, it is evident from Fig. 1 that a simple straight-line extrapolation of the latitudinal extent of the sector region fails deep into the heliosheath, especially in the north. This could explain why early in 2009 Voyager 1 seemed to be in a unipolar region while later in 2009 Voyager 1 reentered the sector region (Burlaga & Ness 2010).

As mentioned earlier, we predict (Drake et al. 2010) that in the heliosheath, near the heliopause the magnetic fields in the sector region will reconnect, forming nested magnetic

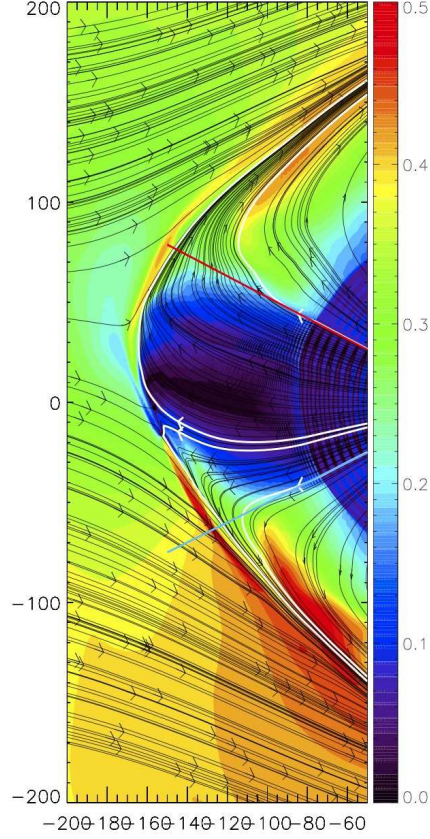


Fig. 1.— Meridional cut from a 3D MHD simulation showing the magnitude of the magnetic field (nT). The sector region of width of 60° is the blue-black region. The flow streamlines are shown in black. The boundary of the sector region is shown in the white streamlines. The Voyager 1 trajectory is 30° above the solar equator and that of Voyager 2 is 29.8° below the solar equator and are shown, respectively, in the red and blue lines.

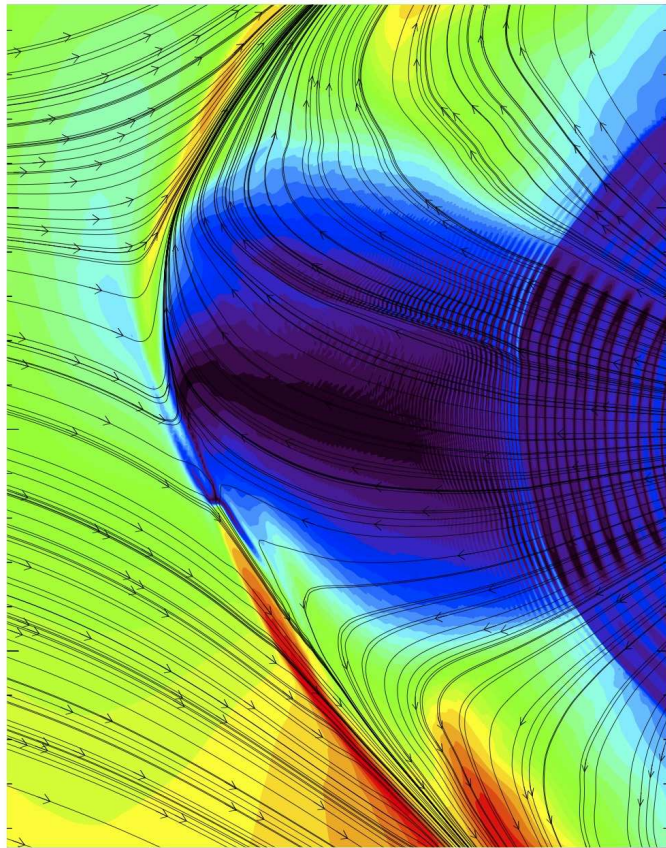


Fig. 2.— A blowup of the sector region of Figure 1

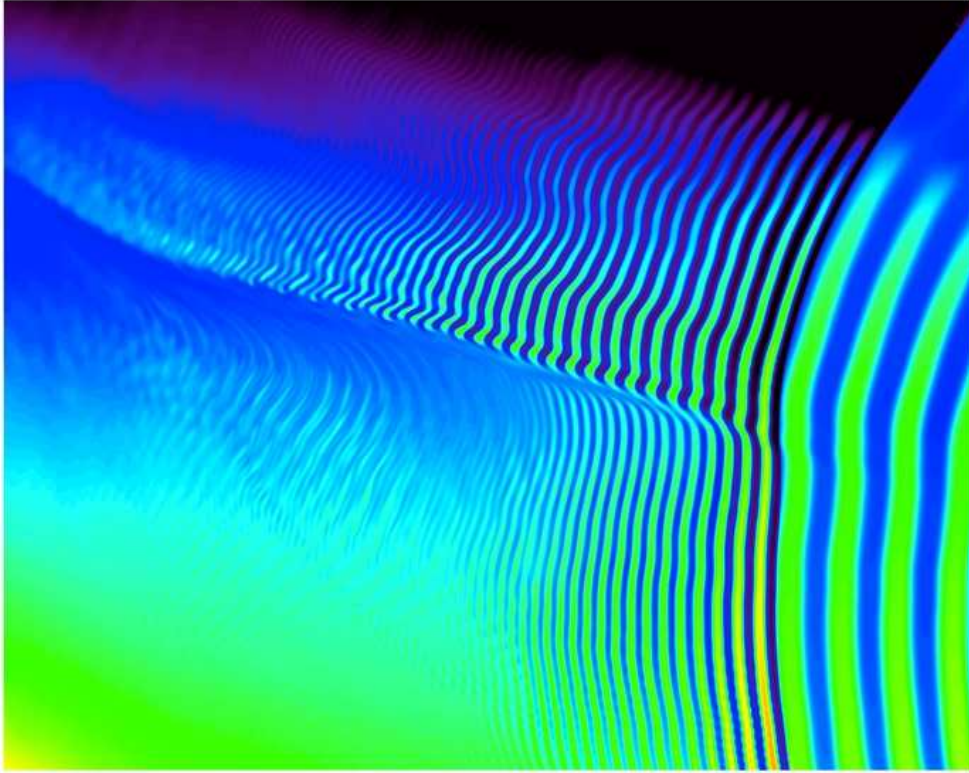


Fig. 3.— A zoom of the sectors between the region just upstream of the termination shock into the heliosheath. The decrease in the spacing of the sectors can be seen as the solar wind crosses the termination shock. The loss of resolution deep in the heliosheath can be seen as well.

islands. We expect the reconnection to be most robust close to the heliopause. On the other hand, the perturbations of the sector structure due to reconnection near the heliopause will cause compressions of the current sheets upstream, possibly triggering reconnection there. The heliosheath flows will carry the magnetic islands/bubbles within the sector region to higher latitudes. Because the dominant heliosheath flow is northward, we therefore predict an asymmetry of the magnetic structure between the northern and southern hemispheres.

3. Observations of Voyager 1 and 2 that Support our Scenario

We present Voyager 1 and 2 data that support our disordered field scenario in Figures 4, 5 and 6. The shaded gray regions are the unipolar regions and the unshaded regions (beyond 2008) corresponds to the sector region (the proposed bubble region). In Figure 4 are daily averages of the intensity of the magnetic field. In the periods of 2008-2008.2 and 2009.15 on (shaded areas) Voyager 2 had a positive polarity ($\lambda = 270^\circ$) with only infrequent excursions to negative polarities. In the time period of 2009.15 on, the field was 90% in the positive polarity with 10% in the negative polarity. Figure 5 is the daily average of the intensity of electrons from 0.022-0.035 MeV, from 0.035-0.061MeV and 0.35-1.5 MeV. Around the period of 2008-2008.2 and from 2009.15 on (shaded areas), there was a drop of the intensity of electrons as measured by Voyager 2. The drop was especially dramatic after 2009.15. In Figure 6 are 0.2 year averages and standard deviations of the radial flows, The measured unipolar regions (between 2008-2008.2 and 2009.15 and 2009.41) are shaded gray and the conjectured unipolar region (after 2009.41) is shaded light gray. We can see that there is a large increase in the intensity of fluctuations in the sector region (non-shaded) as compared with the unipolar regions (shaded). These observations will be discussed more fully after we present the results of the PIC simulations and associated discussion.

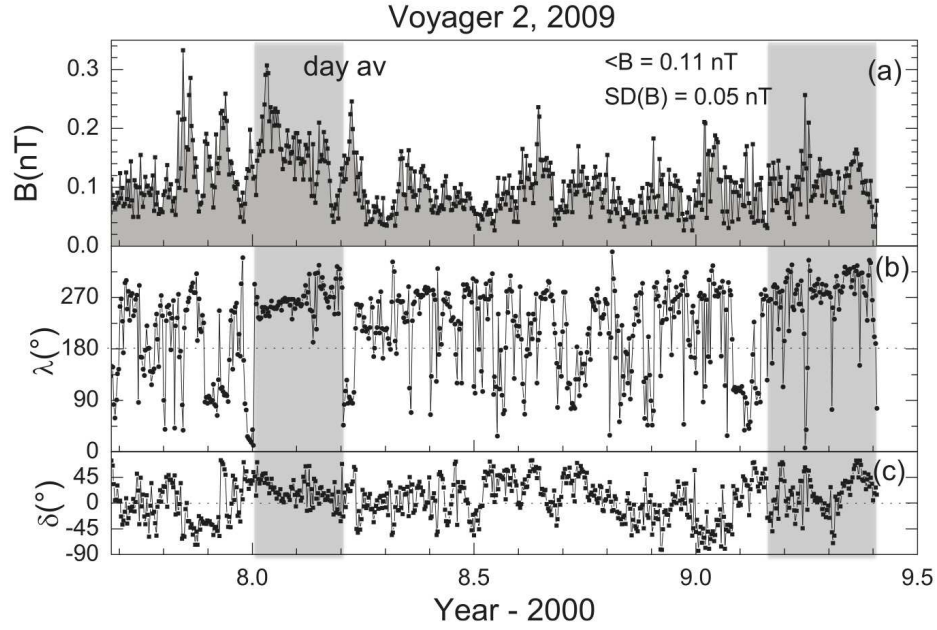


Fig. 4.— Daily averages of the (a) magnetic strength B , (b) azimuthal angle λ , and (c) elevation angle δ measured by Voyager 2. The azimuthal angle λ and the elevation angle δ of B are defined as $\lambda = \tan^{-1}(B_Y/B_X)$ and $\delta = \sin^{-1}(B_z/B)$, where B_X , B_Y , and B_Z are the magnetic field components in the heliographic coordinate system. The unipolar periods between 2008-2008.2 and 2009.15 on, are shaded in gray. The non-shaded regions correspond to the sector region (proposed “bubble” region.) (Courtesy of L. Burlaga.)

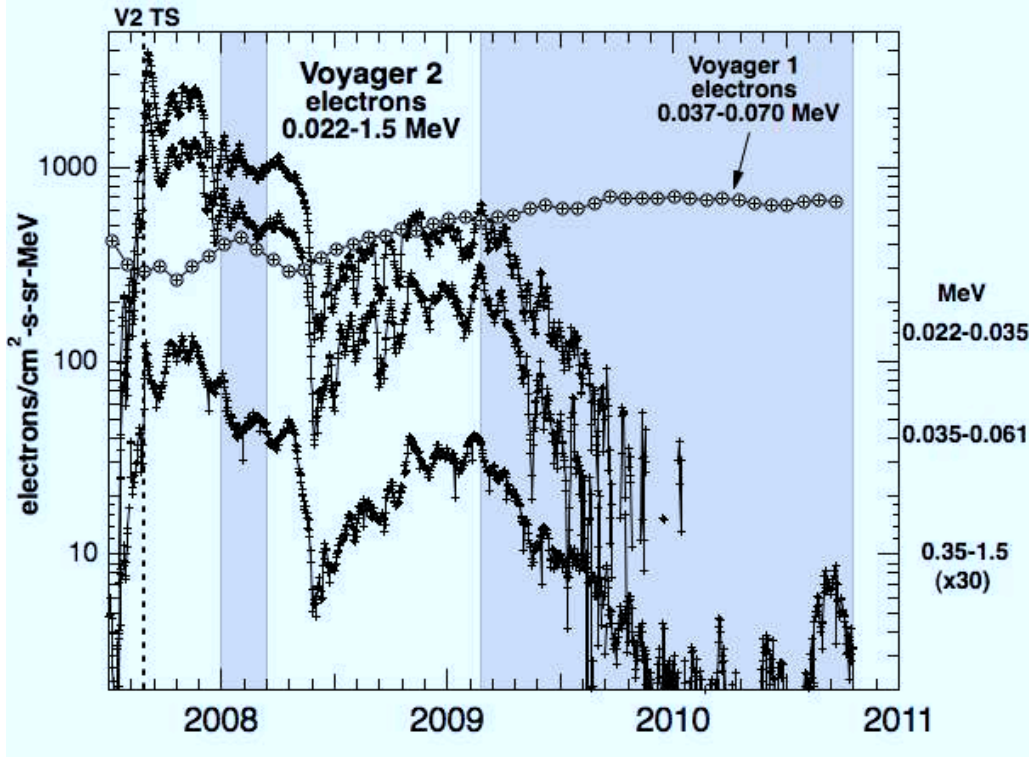


Fig. 5.— Daily average of the intensity of electrons from 0.022-0.035 MeV, 0.035-0.061MeV and 0.35-1.5 MeV. In the unipolar periods around 2008-2008.2 and from 2009.15 on (shaded areas) there is a drop of the intensity of electrons as measured by Voyager 2. The drop was especially dramatic after 2009.15. The non-shaded regions, after 2008, correspond to the sector region (the proposed “bubble” region).

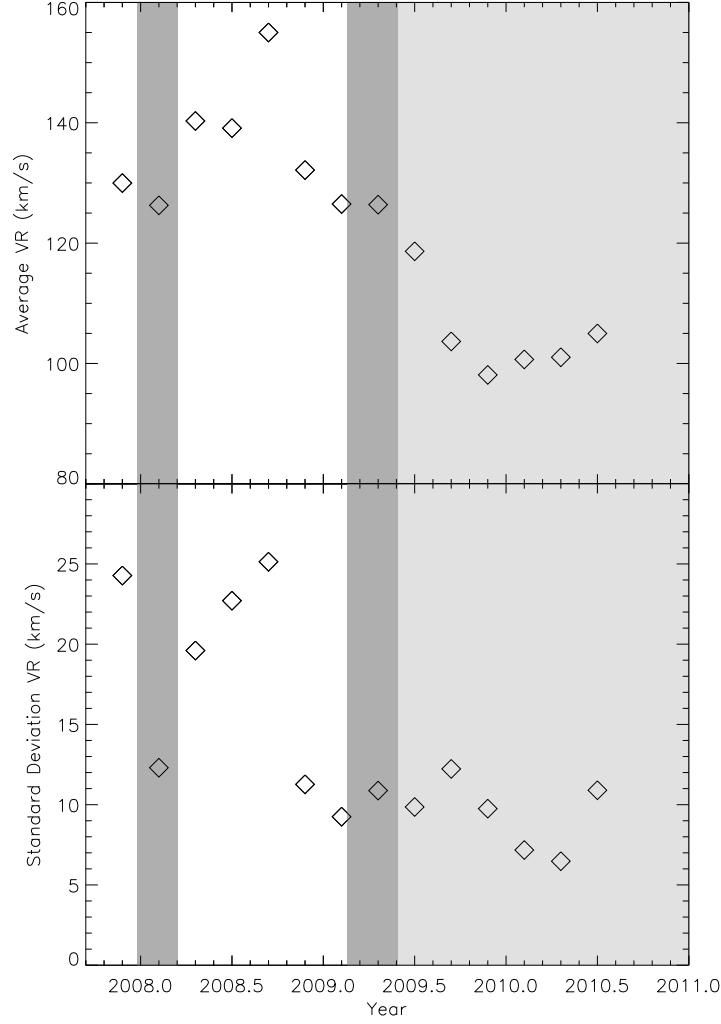


Fig. 6.— a) 0.2 year averages of the radial flows and b) standard deviations of the radial flows as measured by Voyager 2 from 2008.7 to 2010.5. The measured unipolar regions (between 2008-2008.2 and 2009.15 and 2009.41) are shaded gray and the conjectured unipolar region (after 2009.41) is shaded light gray. The non-shaded regions correspond to the sector region (proposed “bubble” region.)

4. Disordered magnetic field in the Heliosheath Sector Region

We also present results from kinetic simulations carried out with the particle-in-cell (PIC) code p3d. The algorithm used is described in detail in Zeiler et al. 2002. Here we present the results of simulations reported earlier in Drake et al. 2010. The initial state had eight current layers, that produced a magnetic field B_x with periodic reversals. Reconnection spontaneously developed and was followed in time. Detailed parameters of these runs were presented in Drake et al. 2010.

As discussed earlier in the Drake et al. 2010 paper, we argued that the compression of the sectors on their approach to the HP would narrow the HCS sufficiently to trigger reconnection of the sector field. In Figures 7a and 8a we show the modulus of the magnetic field B early ($\Omega_p t = 100$) and later ($\Omega_p t = 150$), with Ω_p the proton cyclotron frequency, to illustrate the magnetic topology and the variability of the B as reconnection proceeds. In these simulations y and x correspond to the heliospheric azimuthal and radial directions and d_p is the proton inertial length. The ion flows in the azimuthal direction, v_{py} , are shown at three times in Figure 9, the first two plots correspond to Figures 7 and 8 and the third to $\Omega_p t = 200$. Early in time, the driven outflows from reconnection are evident while later in time, especially by $\Omega_p t = 200$, the flows are erratic and do not exhibit classical reconnection signatures. In Figure 10 are the three components of the ion velocity, tangential (dotted), radial (solid) and normal (dashed) along a cut at $y = 240d_p$ at a time $\Omega_p t = 200$. This is the same time as the 2-D plot of v_y shown in Fig. 9c. The absence of reconnection at late time is not because the magnetic free energy has been completely depleted. Cuts through the simulation along the radial direction (at $y = 240d_p$) in Figures 7b and 8b show B and the heliospheric elevation angle (defined as the angle between the magnetic field and radial direction). Even late in time substantial magnetic energy remains. Further, a casual glance at the behavior of λ might suggest that the sectors are still intact, although with

a more irregular spacing than earlier. These “sectors”, however, correspond to magnetic islands, whose size is comparable to the original sector spacing. The absence of ongoing reconnection is a consequence of firehose stability: the interior of these islands is at the marginal firehose condition ($1 - 4\pi(P_{\parallel} - P_{\perp})/B^2 = 0$), where P_{\parallel} and P_{\perp} represent the parallel and perpendicular components of the pressure), where the magnetic tension that drives reconnection goes to zero (Drake et al. 2006, 2010). Thus, the predicted late-time structure of the sectorized field consists of nested islands with irregular spacing but with scale sizes comparable to the original sector spacing. The remnant flows are erratic and do not exhibit the classic reconnection signatures.

A fundamental question is therefore how far upstream from the HP the nested-island, disordered field extends. While we argued in Drake et al. 2010 that reconnection would only onset close to the HP where the thickness of the HCS could approach d_p , it is possible the reconnection near the HP could spread upstream as the jostling of reconnected islands propagates upstream.

A theoretical exploration of the upstream spread of reconnection in the sectorized field is beyond the scope of the present paper. We argue, however, that the Voyager 2 satellite data presented in Section III provides substantial support for the idea that the sectorized field encountered by Voyager 2 has already undergone reconnection and that the measured magnetic field is in the disordered state shown in Figure 8. The irregular “sector” structure seen in the data corresponds to the irregular magnetic island spacing of Figure 8. The near absence of classic reconnection signatures in the plasma flows in the Voyager data is consistent with their absence in the simulation data. Moreover, at least one reconnection site has been identified in the Voyager 2 data (Burlaga & Ness (2009)) (the presence of *D-sheets* was interpreted as evidence for reconnection (Burlaga & Ness 1968)) that implies the existence of the occasional reconnection event at late time when the magnetic islands

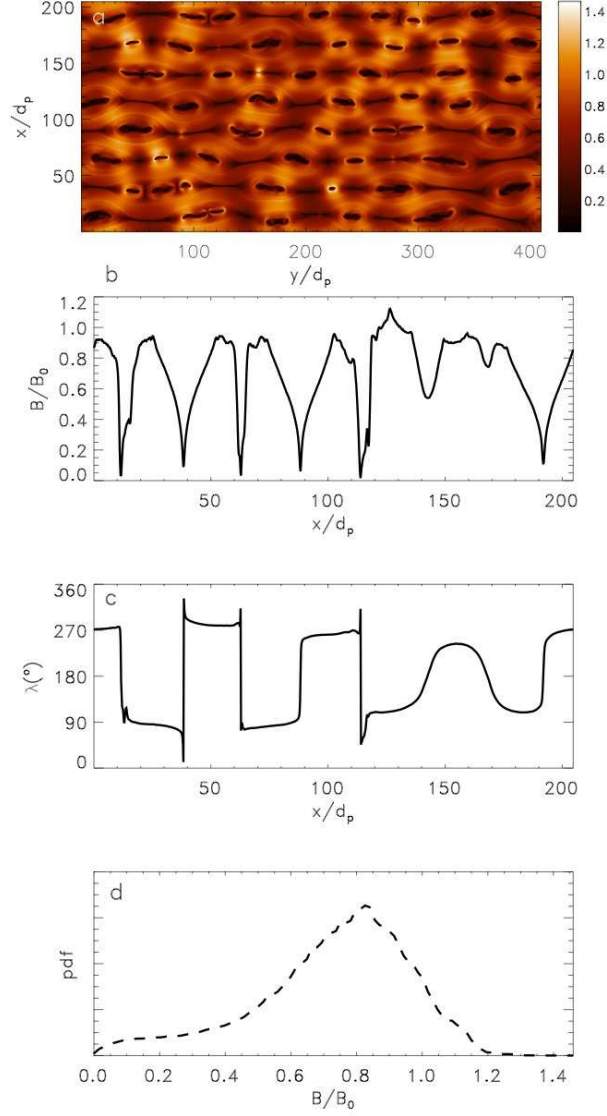


Fig. 7.— Magnetic field structure at $\Omega_p t = 100$ from the PIC simulation described in Drake et al. (2010) where the initial state had $\beta = 0.2$. Panels (a) show the magnitude of the magnetic field B during reconnection of the sectors; (b) the magnetic field intensity in a cut along $y = 240 d_p$; (c) angle λ along $y = 240 d_p$ and (d) the distribution of the magnetic field from the simulation (dashed line).

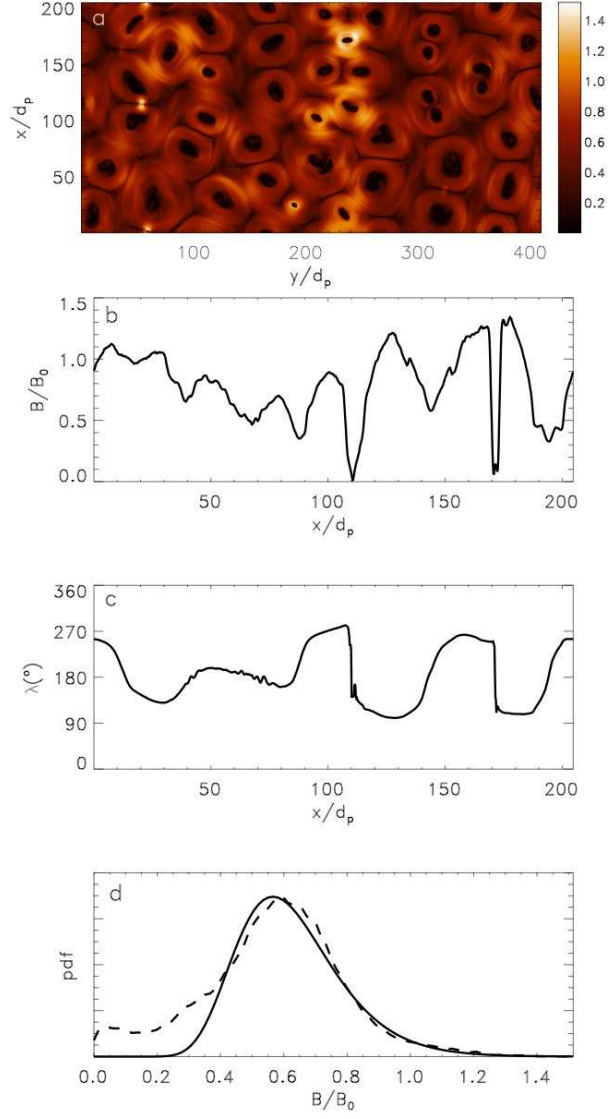


Fig. 8.— Same as Figure 7 but at $\Omega_p t = 150$. The solid line in (d) is a log-normal distribution.

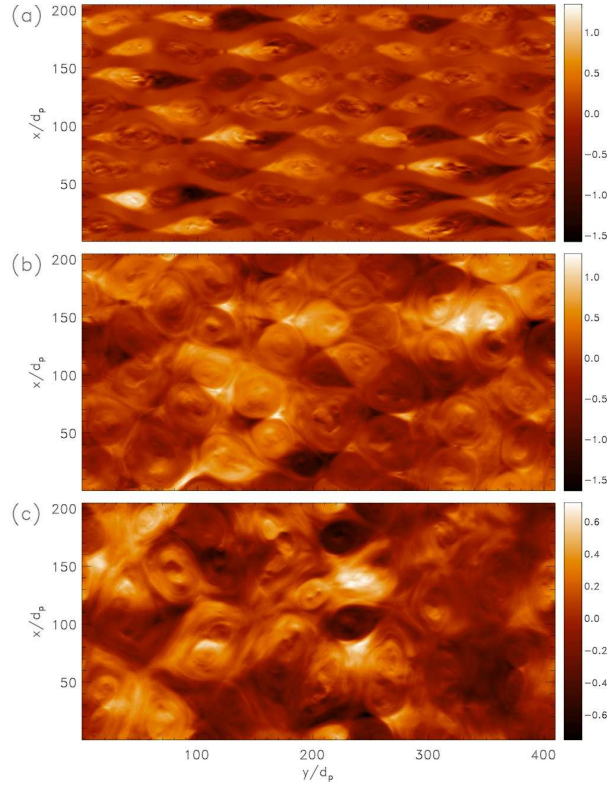


Fig. 9.— Flows of the protons in the azimuthal direction (v_{py} at three times ($\Omega_p t = 100, 150, 200$.)

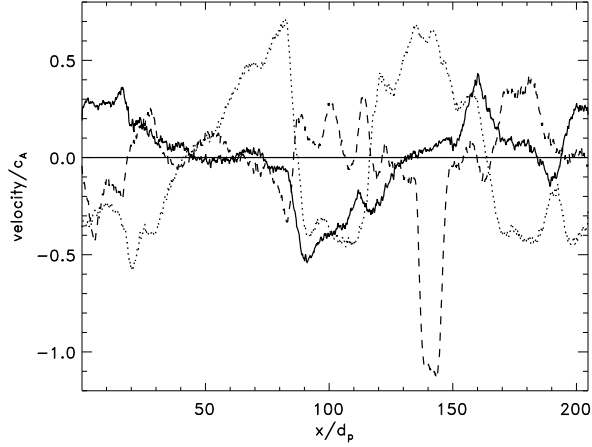


Fig. 10.— Three components of the ion velocity, tangential (dotted), radial (solid) and normal (dashed) along a cut at $y = 240d_p$ at a time $\Omega_p t = 200$. This is the same time as the 2-D plot of v_y shown in Fig. 9c.

merge. Further, the enhanced amplitude of fluctuations in the radial flow data in the “sectored” region compared to unipolar regions (Figure 6) suggests reconnection as the source of the irregular flows. No other driver for these flows, which appear only in the “sectored” region, has been proposed.

The distribution of the azimuthal angle λ is another indicator of a bubble stage. We plot in Figure 11 the distribution of λ for two periods: a) Days 0-65 of 2001 where Voyager 2 was immersed in a sector region (Burlaga et al. 2003) upstream of the termination shock; and b) between 2008.3 to 2009 downstream of the termination shock. We did not include data where the magnitude of the magnetic field was $< 0.05nT$ because, as noted by Burlaga et al. 2010, this is approaching the resolution limit of the magnetometer. Period (b) is representative of a period where we argue that the sector region is in a bubble state. We expect that, similar to Figure 8, λ would be less organized than in the regular sector region (period (a)). This can be seen in Figure 11. The distribution is broader in period *b* than in period *a*.

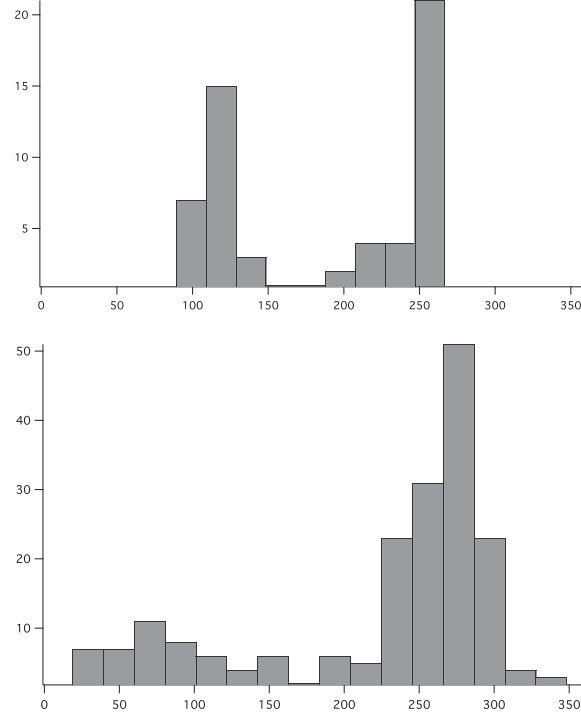


Fig. 11.— Distribution of the azimuthal angle λ in a normal sector (a) and a bubble period (b): a) Days 0-65 of 2001 where Voyager 2 was immersed in a sector region (Burlaga et al. 2003); and b) between 2008.3 to 2009. We did not include data where the magnitude of the magnetic field was $< 0.05nT$ because this is approaching the resolution limit of the magnetometer.

A final piece of evidence in favor of a disordered magnetic field concerns the probability distribution of the magnetic field strength measured by Voyager 2. In the sector region the probability distribution has been empirically found to be log-normal, while it appears Gaussian in unipolar regions. The distribution of B from the PIC simulations is shown in Figures 7d and 8d. Early in time, the distribution does not match an obvious form. However, at late time the distribution of B from the simulation (dashed line) matches a log-normal (solid line) surprisingly well at large B . The match is not good at small B . The discrepancy at small B may be because the initial magnetic distribution consisted of simple anti-parallel fields while in reality the field rotates in the reversal region so there are no regions of zero field (Smith et al. 2001). In the simulations the tail of high magnetic fields arises as the magnetic bubbles, which exhibit substantial motion even after reconnection has largely ended (see Figs. 9c and 10), bounce off one another, compressing magnetic flux lying between the colliding bubbles (white regions of Figure 8a). This behavior can be most clearly seen in movies of the 2-D evolution of B (not shown). This behavior does not take place during the reconnection phase of the initial current sheets (Figures 7 b,c).

The heliosheath magnetic field data from Voyager 1 also supports the idea that the heliosheath field in the sector region has already reconnected. During the 2007.4-2008.2 time period (Burlaga et al 2009b) the spacecraft was in a region of negative polarity, indicating that it was outside of the sector region in the region of northern polarity. During this time the fluctuations in magnetic field strength dropped significantly compared to time intervals when the spacecraft was in the sector region. The higher level of fluctuations in the sector region is consistent with that expected from the nested-bubble state after reconnection of the sector field (Fig. 9). Finally, in 2009, in day 254 (Burlaga & Ness (2010)) Voyager 1 entered into a region of positive polarity and remained there through the remainder of 2009. Presumably the spacecraft was in the sector region during this period but due to the radial flow in the heliosheath remained in a single sector. During

this time period the magnetic field data exhibited a high level of fluctuations: the magnetic field statistics during all of 2009 exhibited a log-normal distribution (with a pronounced tail of high magnetic field events) while during the period 1-254 exhibited a more Gaussian distribution. Again these observations suggested that the sector region in the vicinity of Voyager 1 is in a disordered state.

An important question is why even when leaving the sector region for brief periods (e.g., during 2006.2), the intensity of the low energy electrons did not drop at Voyager 1 (Figure 5)? We believe that this is because the much thicker sector region in the northern hemisphere compared with that in the southern hemisphere (Figure 1): the thicker sector region in the north is a much stronger source of energetic electrons than that in the south and is able to maintain a high flux of the electrons even in the unipolar region. Confirmation of this hypothesis will require a careful modeling effort taking into account the disordered field in the outer heliosphere.

The evolution of the reconnection in a sector field depends strongly on the β =thermal pressure/magnetic pressure of the initial plasma. At higher values of β reconnection is dominated by longer wavelength modes and island contraction quickly causes the plasma within islands to hit the marginal firehose condition, which suppresses reconnection (Schoeffer et al. 2011). As a result, the islands at late time in the high β case remain elongated rather than nearly round as in the case of low β . This difference can be seen by comparing the geometry of islands at late time for the $\beta = 0.2$ initial state (Fig. 8a) versus that for $\beta = 4.8$ (Fig. 12a). The high β case continues to exhibit regions of intense magnetic field (Figs. 12a, b) and the distribution of B again takes the form of a lognormal distribution (Fig. 12d).

The round versus elongated structure of bubbles at late time has a dramatic impact on the distribution of λ and therefore offers an important clue about the late time magnetic

structure of the heliosheath. A cut of λ for $\beta = 4.8$ is shown in Fig. 12c. The differences in the λ distributions for the low and high β can be most clearly seen in the distribution of λ averaged over the entire computational domain (Fig. 13). Shown in Fig. 13a is the data for the $\beta = 0.2$ initial state and in Fig. 13b is that for the $\beta = 4.8$ initial state. The distribution of λ for the $\beta = 0.2$ case has peaks at $0^\circ/360^\circ$ and 180° while for the $\beta = 4.8$ case it peaks around 90° and 270° but with a broad distribution. The distribution of λ at $\beta = 4.8$ is similar to the Voyager 2 data in the hypothesized bubble region. The value of β in the heliosheath is unknown, but there are indications that it is high due to the contributions from the suprathermal population of pickup ions.

5. Discussion

Our prediction is that there will be an asymmetry between the northern and southern hemisphere with respect to the structure of the heliospheric magnetic field close to the heliopause. In the northern hemisphere and to less extent in the southern hemisphere there will be a disordered field resulting from reconnection of the sectors. Additionally, we predict that upstream of the heliopause, but within the sector region the magnetic field will be disordered as well (see Figure 14.). The present PIC simulations are 2D, in the plane of the reversals of the magnetic field. This plane corresponds to the azimuthal plane in 3D, or in the xy plane in Figure 14. The structure and dynamics of the bubbles in 3D is an issue that will be explored in a future work.

Energetic electrons are especially sensitive to the topological structure of magnetic fields. The presence of magnetic islands/bubbles can significantly impact the transport of energetic electrons (and ions) in the heliosheath compared with that in a laminar region. While in a laminar field, the transport is dominated by field-aligned motion in longitude; magnetic islands/bubbles in the x-y plane strongly inhibit such motion. In the disordered

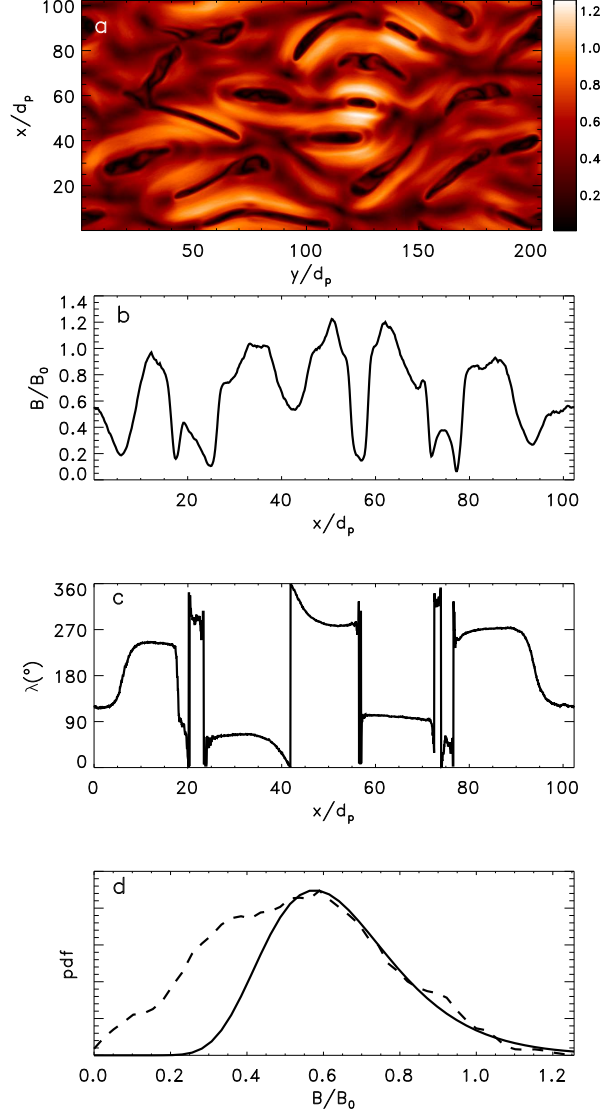


Fig. 12.— Same as Figure 8 for a case with $\beta = 4.8$ in the initial state. The panels (b) and (c) show cuts along x for $y = 127.5d_p$. The solid line in (d) is a log-normal distribution.

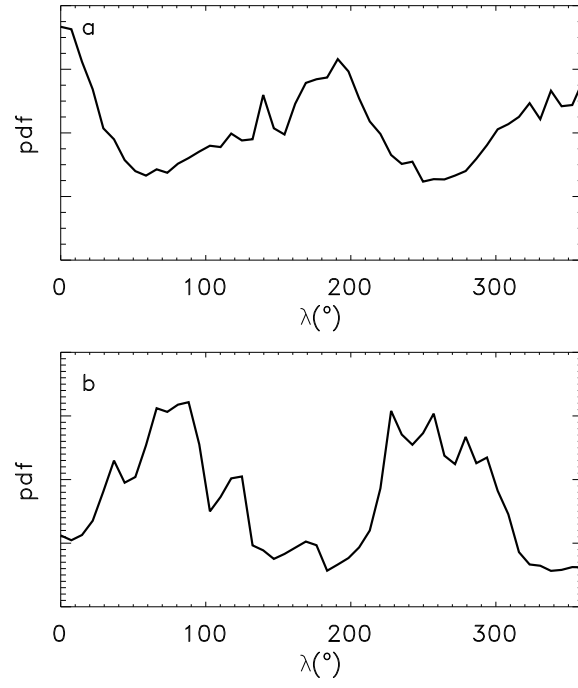


Fig. 13.— The distribution of λ over the entire simulation domain for initial conditions with (a) $\beta = 0.2$ and (b) $\beta = 4.8$.

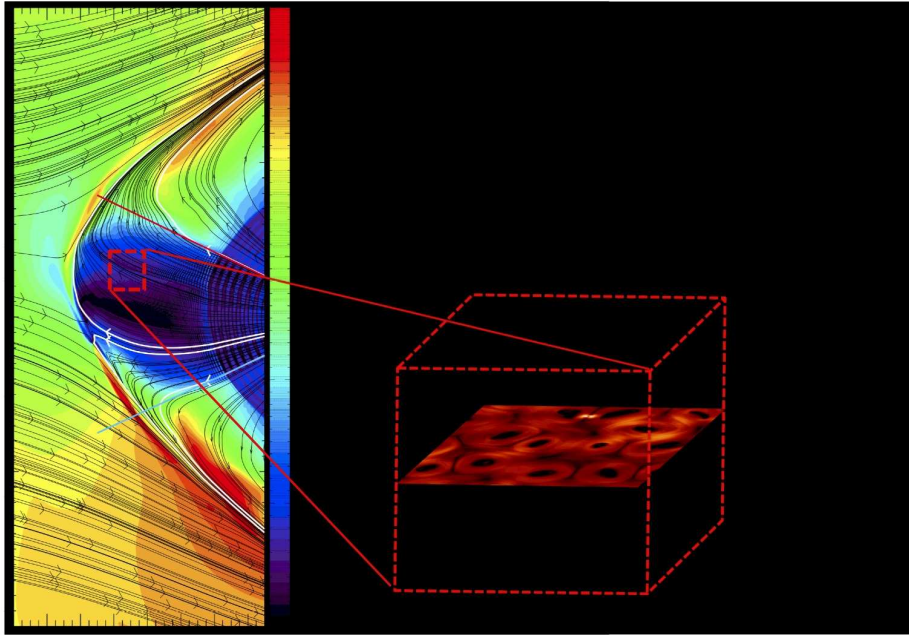


Fig. 14.— Representation of what we expect the outer heliosphere to be: a bath of bubbles. The plane from the MHD simulation is a meridional plane, a x - z plane. The PIC simulation was done in the azimuthal plane, the x - y plane.

field in the northern hemisphere (and the part that was carried to the south) convective transport may compete with field aligned streaming in controlling the spatial distribution of electrons (and ACRs).

We predict that the electrons and ions accelerated in the heliosheath close to the heliopause will have much different transport characteristics in a disordered sector field in comparison with the laminar field in the unipolar region. The electrons (and ions) will be locally trapped on magnetic islands in a reconnected sector region and will make their way through the heliosheath in a complex diffusion process: magnetic islands will act as local storage vessels for energetic particles. Once the electrons are in a region of ordered field they will rapidly escape. Upstream of the termination shock and at latitudes above and below the sector boundary the field retains its nominal laminar Parker structure. Once the electrons access the Parker field they rapidly escape towards the inner heliosphere. The termination shock and the sector boundaries therefore act as sinks for energetic electrons. We would expect the energetic electron population in the heliosheath to be much larger than that upstream of the termination shock, which is what is observed.

The observations support this scenario. From Figure 4 we argue that Voyager 2 crossed into a region of unipolar field in the period of 2009.15 onward (90% of the time the field was negative from 2009.15-2009.4). In the period between 2008-2008.2 Voyager 2 also crossed into a unipolar region. These two periods (shaded areas) correspond to a drop of intensity of electrons in the energy range (0.02-1.5 MeV) measured by Voyager 2 while the energetic electrons at Voyager 1 remained at the same level or even increased (Figure 5). These two periods also coincide with the periods when the fluctuations of the radial flows as measured by Voyager 2 were low, as seen in Figure 6. This is evidence that in these periods Voyager 2 left a region of disordered field where they were trapped within magnetic islands. The electrons then accessed the laminar Parker field and rapidly escaped. We further expect

some anisotropy of electrons before and after mid 2009.15 on the Low Energy Charged Particle Experiment (LECP).

The disordered heliospheric magnetic field near the heliopause will affect the entrance and modulation of galactic cosmic ray (GCR) electrons making the northern hemisphere more “transparent”. The GCR electrons travelling along the interstellar magnetic fields can enter and percolate through the heliosphere. The ones entering the northern hemisphere will travel through the disordered field of the sector region, while those in the southern hemisphere will access a laminar field more quickly and escape. We expect therefore a north-south asymmetry in the intensity and modulation of the GCR electrons.

This picture is in agreement with the observations of (McDonald 2010), which exhibit a dramatic asymmetry between Voyager 1 and 2 in the intensity of GCR electrons with energies of 3.8-59 MeV. The intensities at Voyager 1 continue to rise while those at Voyager 2 reached a plateau well “below” that of Voyager 1.

As described above, our scenario predicts that the transport of particles will be different inside and outside the sector region. In particular, it predicts that independent of the solar cycle there should be an increased source of GCRs and energetic electrons at lower latitudes. The energetic electrons and GCR entering the heliosphere will percolate through the bubbles until leaving the sector region and quickly migrating into the inner heliosphere.

This scenario will affect as well our understanding of reconnection at the heliopause where we argued that the most favorable location for reconnection was where the interstellar magnetic field was antiparallel to the heliospheric field (Swisdak et al. 2009). In that work we assumed that the heliosheath field was laminar with a organized polarity in each hemisphere. What happens when a laminar interstellar magnetic field approaches a sea of magnetic islands needs to be investigated.

The sector region is carried to the north so Voyager 1 is expected to remain inside the sector region all the way to the heliopause. Voyager 2 after leaving the sector region in 2009.15 is expected to eventually re-enter the sector region, but at a radial location much closer to the heliopause.

In this work mainly we focused on the energetic electrons. However, we expect that because of the north-south asymmetry of the sector region there will be an asymmetry in the intensity of the ACRs between Voyager 2 in the southern hemisphere and Voyager 1 in the northern hemisphere. This should be more visible as the HCS moves to lower latitudes than Voyager 2. Current analysis of the data does not reveal the spatial intensity gradients because the ACRs are dominated by temporal variations (Decker et al. 2009). Future study will have to disentangle the temporal variation in order to confirm our prediction of a gradient between Voyager 1 and 2.

M. O. would like to acknowledge the support of NASA-Voyager Guest Investigator grant NNX07AH20G. This work is also supported by the National Science Foundation CAREER Grant ATM-0747654. J. D. and M. S. were supported by the grant ATM-0903964. M. O. would like to thank especially the staff of NASA Supercomputer Division at Ames and the Pleiades award SMD-10-1600 that allowed the simulations to be performed. The PIC simulations were carried out at the National Energy Research Super Computer Center (NERSC). Work at JHU/APL was supported by the NASA Voyager Interstellar Mission, Contact NNX07AB02G. This research benefited greatly from discussions that were held at the meetings of the International Team devoted to understanding the -5 tails and ACRs that has been sponsored by the International Space Science Institute in Bern, Switzerland.

REFERENCES

- Alexashov, D. & Izmodenov, V. V. Kinetic vs. multi-fluid models of H atoms in the heliospheric interface: a comparison. *Astron. & Astrophys.* 439, 1171-1181 (2005).
- Burlaga, L. F., & Ness, N. F., *Can. J. Phys.*, 46, 1962 (1968).
- Burlaga, L. F., Ness, N. F., & Richardson, J. D., *Journal of Geophys. Res.* 108, NO. A10, 8028, doi:10.1029/2003JA009870 (2003)
- Burlaga, L. F., Ness, N. F., *Astrophysical Journal*, 703, 311 (2009).
- Burlaga, L. F., Ness, N. F., Acua, M. H., Richardson, J. D., Stone, E., McDonald, F. B., *Astrophysical Journal*, 692, 1125 (2009a).
- Burlaga, L. F., Ness, N. F., Acuna, M. H., Wang, Y.-M., and Sheeley Jr., N. R., *Journal of Geophys. Res.* 114, A06106, doi:10.1029/2009JA014071 (2009b)
- Burlaga, L. F., Ness, N. F., Wang, Y., -M., Sheeley, N. R., Richardson, J. D. *Journal of Geophys. Res.* 115, A08107, doi:10.1029/2009JA015239 (2010).
- Burlaga, L.F., Ness, N.F., *Astrophysical Journal*, in press (2010).
- Borovikov, S., Pogorelov, N., Zank, G., Kryukov, I. American Geophysical Union, Fall Meeting 2008, abstract SH21B-1600
- Czechowski, A., Strumik, M., Grygorczuk, J., Grzedzielski, S., Ratkiewicz, R. and Scherer, K., *Astronomy and Astrophysics* 516, A17 (2010).
- Decker, R. B., Krimigis, S. M., Roelof, E. C., and Hill, M. E., AIP, 8th Annual International Astrophysics Conference, CSPAR (2009).
- Decker, R. B., Krimigis, S. M., Roelof, E. C., and Hill, M. E., AIP, 9th Annual International Astrophysics Conference, CSPAR, in press (2010).

- Drake, J., Opher, M., Swisdak, M., Chamoun, J. N., *Astrophysical Journal* 709, 963 (2009).
- Fisk, L. A., & Gloeckler, G., *Astrophysical Journal*, 640, L79 (2006).
- Heerikhuisen, J. *et al.* *Astrophysical Journal*, 708, L126 (2010).
- Izmodenov, V. V., *Space Sci. Rev.* 143, 139-150 (2009).
- Lazarian, A., Opher, M., *Astrophysical Journal* 703, 8 (2009).
- McComas, D., & Schwadron, N. A., *Geophysical Research Letters*, Volume 33, Issue 4 (2005).
- McComas, D. J., *et al.* *Science* 326, 959 (2009).
- McDonald, F., private communication (2010).
- McComas, D. J., *et al.* *Science*, 326, 959 (2009).
- Opher, M., Stone, E. C., Liewer, P. C., *Astrophysical Journal*, 640, L71, (2006).
- Opher, M., Stone, E. C., Gombosi, T. I., *Science* 316, page 875, (2007).
- Opher, M., Alouani Bibi, F., Toth, G., Richardson, J. D., Izmodenov, V. V., Gombosi, T. I., *Nature* v. 462 1036 (2009).
- Opher, M. *et al.* in preparation (2011).
- Pogorelov, N. V., *et al.* (2007), in *Turbulence and Nonlinear Processes in Astrophysical Plasmas: 6th Annual International Astrophysics Conference*, AIP Conf. Proc., 932, 129 136, doi:10.1063/ 1.2778955.
- Pogorelov, N.V., Heerikhuisen, J., & Zank, G. *ApJ*, 675, L41.
- Ratkiewicz, R. & Grygorczuk, J., *Geophysical Research Letters*, Volume 35, Issue 23 (2008).

- Richardson, J. D., Kasper, J. C., Wang, C., Belcher, J. W., & Lazarus, A. J., *Nature*, 454, 63 (2008).
- Schoeffler, K. et al. in preparation (2011).
- Smith, E. J., The heliospheric current sheet, *J. Geophys. Res.*, 106, 15,819-15,831, doi:10.1029/2000JA000120 (2001).
- Stone, E. C., Cummings, A. C., McDonald, F. B., Heikkila, B. C., Lal, N., & Webber, W. R., *Science*, 309, 2017 (2005).
- Stone, E. C., Cummings, A. C., McDonald, F. B., Heikkila, B. C., Lal, N., & Webber, W. R., *Nature*, 454, 71 (2008).
- Swisdak, M., Opher, M., Drake, J., Alouani-Bibi, F., *Astrophysical Journal* 710, 1769-1775 (2010).
- Toth, G., et al, *Journal of Computational Physics*, in press (2011).
- Zank, G. P., Pauls, H. L., Williams, L. L. & Hall, D. T., *J. Geophys. Res.* 101, 21639-21655 (1996).
- Zank, G. P., *Space Science Reviews*, v. 89, Issue 3/4, p. 413-688 (1999).
- Zeiler, A., D. Biskamp, J. F. Drake, B. N. Rogers, M. A. Shay, and M. Scholer (2002), *J. Geophys. Res.*, 107 (A9), 1230, doi:10.1029/2001JA000287.